Helical Flow of Power-Law Fluids

M. Dostál, R. Žitný, and J. Šesták
Czech Technical University of Prague, Faculty of Mechanical Engineering, Technická 4, 166 07 Prague 6, Czechoslovakia

M. Houška
Food Industry Research Inst., Radiová 7, 102 31 Prague 10, Czechoslovakia

Introduction

Helical flow of non-Newtonian fluids in an annular gap is encountered in mechanical equipment such as deep well drilling or in production lines for extrusion of artificial casings. Although fundamental theory and relations for this type of flow was given by Coleman and Noll (1959), a general solution is not available. Dierckes and Schowalter (1966) applied their theoretical results for the flow of a power-law fluid without stating the equations explicitly. Rea and Schowalter (1967) verified the theoretical predictions experimentally with one fluid obeying the power-law approximation. Bird et al. (1977) presented an asymptotic solution for thin gaps and arbitrary values of the flow behavior index. Wronski et al. (1988) presented results of calculations valid for a limited range of the radii ratio only.

Dostál (1990) recently solved numerically the problem for radii ratio in the range 0.1–0.95 and flow behavior index 0.1–1.0.

The main goal of this work is to present the detailed numerical solution of the helical flow of the power-law fluid for any cylinder radii ratio and arbitrary flow behavior index and the experimental test of the theory.

Theory

The geometry of the flow is shown in Figure 1. For a steady and fully developed isothermal creeping flow, the momentum balance equations in the tangential and axial directions reduce to:

$$0=\frac{1}{r^2}\frac{d}{dr}(r^2\tau_{r\varphi}) \tag{1}$$

$$0=\frac{\Delta p}{L}+\frac{1}{r}\frac{d}{dr}(r\tau_{rz}) \tag{2}$$

Stress components $\tau_{r\varphi}$ and τ_{rz} may be expressed from the generalized power-law model as:

$$\tau_{r\varphi}=m\left[\left(r\frac{d}{dr}\left(\frac{v_\varphi}{r}\right)\right)^2+\left(\frac{dv_z}{dr}\right)^2\right]^{\frac{n-1}{2}} r\frac{d}{dr}\left(\frac{v_\varphi}{r}\right) \tag{3}$$

$$\tau_{rz}=m\left[\left(r\frac{d}{dr}\left(\frac{v_\varphi}{r}\right)\right)^2+\left(\frac{dv_z}{dr}\right)^2\right]^{\frac{n-1}{2}}\frac{dv_z}{dr} \tag{4}$$

where m and n stand for the consistency and flow behavior index of the fluid respectively.

The corresponding boundary conditions are as follows:

$$v_\varphi(r)\,|_{r=R_1}=v_0 \tag{5}$$

$$v_\varphi(r)\,|_{r=R_2}=0 \tag{6}$$

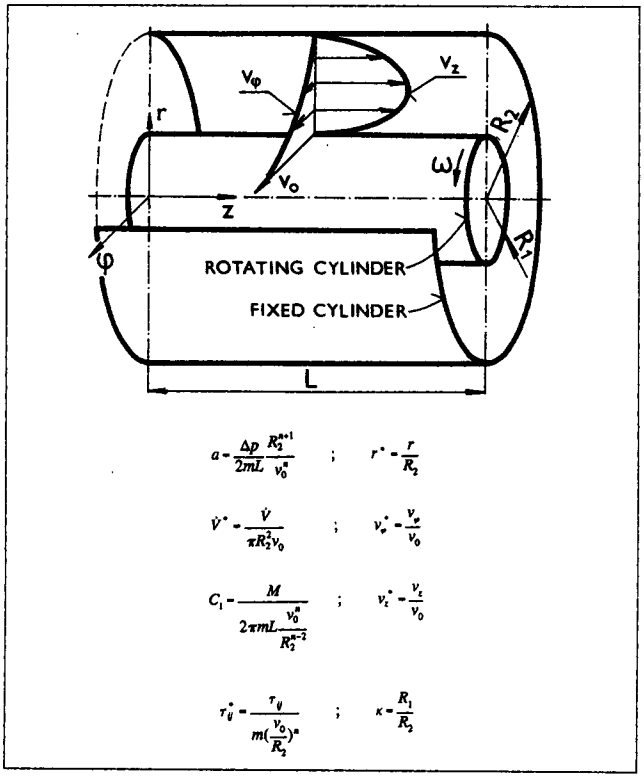

Figure 1. Geometry of helical flow and definition of dimensionless quantities.

$$v_z(r)|_{r=R_1}=0 \tag{7}$$

$$v_z(r)|_{r=R_2}=0 \tag{8}$$

The mathematical formulation has been transformed into a dimensionless form using variables given in Figure 1. Equations 3 and 4 were substituted into Eqs. 1 and 2 and integrated with C_1, C_2 as constants of integration. C_1 was found to be a dimensionless torque acting on the inner cylinder. The integration constant C_2 was quite formally replaced by λ through the relation:

$$\lambda^2=\frac{C_2}{a} \tag{9}$$

The value of λ identifies the dimensionless radial variable r^* location where $dv_z/dr=0$, that is, the maximum axial velocity position in the gap.

After solving this system of equations for the velocity gradients and another integration, the dimensionless velocity components were found to be:

$$v_\varphi^*=r^*\int_\kappa^{r^*}\frac{C_1}{r^{*3}}\left[\frac{C_1^2}{r^{*4}}+a^2\left(r^*-\frac{\lambda^2}{r^*}\right)^2\right]^{\frac{1-n}{2n}}dr^*+C_3r^* \tag{10}$$

$$v_z^*=$$

$$-a\int_\kappa^{r^*}\left(r^*-\frac{\lambda^2}{r^*}\right)\left[\frac{C_1^2}{r^{*4}}+a^2\left(r^*-\frac{\lambda^2}{r^*}\right)^2\right]^{\frac{1-n}{2n}}dr^*+C_4 \tag{11}$$

Integration constants C_1, λ, C_3 and C_4 were determined using dimensionless equivalents of boundary conditions in Eqs. 5-8. From the requirements on the rotating cylinder, Eqs. 5 and 7:

$$C_3=\frac{1}{\kappa} \tag{12}$$

$$C_4=0 \tag{13}$$

whereas for the no-slip conditions in Eqs. 6 and 8 on the surface of the outer cylinder Eqs. 10 and 11 yield:

$$0=\int_\kappa^1\frac{C_1}{r^{*3}}\left[\frac{C_1^2}{r^{*4}}+a^2\left(r^*-\frac{\lambda^2}{r^*}\right)^2\right]^{\frac{1-n}{2n}}dr^*+\frac{1}{\kappa} \tag{14}$$

$$0=\int_\kappa^1\left(r^*-\frac{\lambda^2}{r^*}\right)\left[\frac{C_1^2}{r^{*4}}+a^2\left(r^*-\frac{\lambda^2}{r^*}\right)^2\right]^{\frac{1-n}{2n}}dr^* \tag{15}$$

Solving Eqs. 14 and 15 for C_1 and λ, the velocity components are completely determined. The flow rate $\dot{V}$ is calculated from the relation:

$$\dot{V}=2\pi\int_{R_1}^{R_2}rv_z(r)dr \tag{16}$$

or from its dimensionless equivalent:

$$\dot{V}^*=2\int_\kappa^1 r^*v_z^*(r^*)dr^* \tag{17}$$

Results of the numerical solution were checked in several ways. First of all, for Newtonian fluids, the well-known analytical solution incorporating both limiting cases, that is, pure tangential flow for $v_z=0$ and pure axial flow with $v_\varphi=0$, was used as a source of easily computable reference data.

Furthermore, for arbitrary values of n and $\kappa\to1$, that is, for negligible curvature, an asymptotic solution by Bird et al. is available. In all the checked cases, excellent agreement with values obtained numerically was found.

For calculations of the flow rate for a given pressure drop as well as for the inverse problem, on IBM PC XT/AT/386/486 compatible computers, a software package is available.

Results of numerical calculations are presented graphically. The flow rate $\dot{V}^*$ and torque C_1 were plotted as functions of the dimensionless pressure difference a, with the flow behavior index n as a parameter. A typical example of these relations, valid for $\kappa=0.5$ is shown in Figure 2. Graphs for different values of κ in the range $\kappa=0.1$–0.95 and $n=0.1$–1.0 are available on request.

Experimental

Experiments were made on a setup consisting of an adapted rotational rheometer with coaxial cylinders (Rheotest 2) in a $\kappa=0.805$ geometry. The cup of the rheometer was modified such as to enable axial flow through the gap and reliable pressure difference measurement. Details are apparent from Figure 3.

Six different model liquids were used in the experiments. Relevant physical and rheological properties of the model liquids are given in Table 1. Rheological parameters were determined on a commercial Haake RV-3 rheometer. Flow of the model liquid through the gap was secured either by gravity, as shown in Figure 3, or by means of a small centrifugal pump. Flow rate was measured by a volumetric method. Properties of each liquid were measured after passage through the apparatus, at the same temperature.

Theoretical values of the pressure difference a and torque for each set of the measured parameters (temperature, rheological properties, κ, flow rate and inner cylinder rotational speed) were calculated for all the experimental runs.

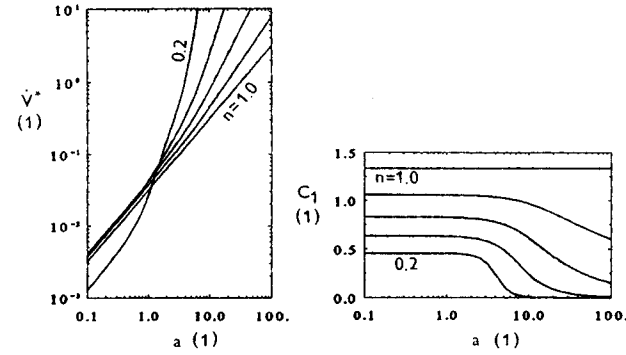

Figure 2. Dimensionless flow rate and torque as a function of dimensionless pressure difference; numerical calculations for $\kappa=0.5$.

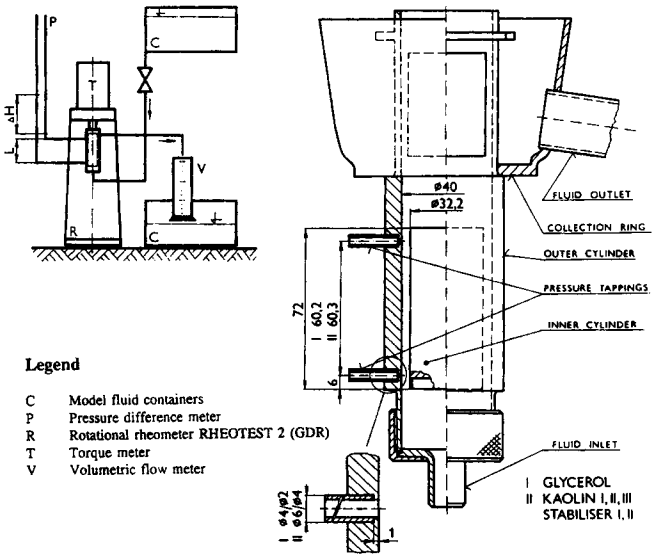

Figure 3. Experimental setup.

All dimensions are given in millimeters.

Results and Discussion

Experimental data of the pressure difference and torque were converted into dimensionless form and compared with theoretical values predicted by the numerical procedure. Results of the comparison are given in Figures 4 and 5.

Very good agreement was found between theoretical and experimental pressure differences. Maximum relative deviation between calculated and measured pressure difference was found to be about $\pm 10\%$.

On the other hand, dimensionless torque values found experimentally were systematically greater than those, calculated theoretically, the maximum relative deviation being $+25\%$. This effect may most probably be explained by the fact that the inner cylinder including its shaft were immersed in the model fluid more than admissible in standard geometrical configurations for which the shear stress constant of the cylinder was calibrated (experimental value of C_1 was determined from the value of shear stress acting on the inner cylinder). Also, the fluid level varied with the flow rate. Consequently, the measurement error was not constant.

Conclusion

It has been confirmed experimentally that the increase of the rotational speed of the inner cylinder enhances the axial flow rate as predicted by the theory for the power-law model. The lower the flow behavior index, the higher enhancement of the flow rate at the same pressure difference was observed. This effect verified the decrease of apparent viscosity as predicted by the power-law model for two-dimensional flow.

For engineering estimates, results of the theoretical analysis are available in graphical form. Graphs valid for κ in the range 0.1–0.95 or a software package are available on request.

Notation

a = $\Delta p R_2^{n+1}/(2mLv_0^n)$ = dimensionless pressure difference, 1
C_1 = $M/[2\pi mL(v_0^n/R_2^{n-2})]$ = dimensionless torque, 1
$\dot{V}^*$ = $\dot{V}/\pi R_2^2 v_0$ = dimensionless flow rate, 1
$\dot{V}$ = flow rate, $m^3 \cdot s^{-1}$
M = torque, N·m
Δp = pressure difference, Pa
R_1 = inner radius, m
R_2 = outer radius, m
v_0 = velocity of the inner cylinder, $m \cdot s^{-1}$
L = length of the annulus, m

Table 1. Model Fluids Characteristics

			Power Law Model Parameters		Power Law Model Accuracy Helical Flow Experiments		
	ρ	t	m	n	$\Delta\tau_{max}/\tau$	$\dot{\gamma}_{min}$	$\dot{\gamma}_{max}$
	$kg \cdot m^{-3}$	°C	$Pa \cdot s^n$	1	%	s^{-1}	s^{-1}
Glycerol	1,242	16.00	0.570	1.000			
Kaolin I	1,224	16.60	2.960	0.350	4.3	10	240
Kaolin II	1,232	18.60	1.410	0.460	5.5	10	240
Kaolin III	1,244	18.80	0.910	0.570	4.6	10	218
Stabilizer I	998	21.90	0.652	0.498	2.7	8	200
	998	22.55	0.641	0.500			
	998	23.70	0.621	0.505	3.3	10	199
Stabilizer II	997	23.70	1.977	0.415	2.2	10	203
	997	24.70	1.923	0.418	1.9	5	202
	997	32.58	1.543	0.445	2.8	10	201
	997	33.68	1.497	0.449	4.0	10	201

wt.%

	Kaolin	Glycerol	Water	Hamulsion*
Glycerol		92.6	7.4	
Kaolin I	17.4	40.3	42.3	
Kaolin II	14.4	49.3	36.3	
Kaolin III	12.3	55.7	32.0	
Stabilizer I			99.5	0.5
Stabilizer II			99.0	1.0

*Hamulsion is the trademark of a food stabilizer and thickener produced by G. C. Hahn & Co., Lubeck, Germany.

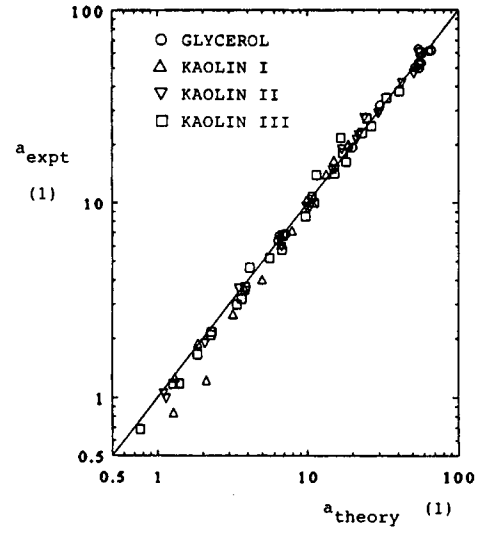

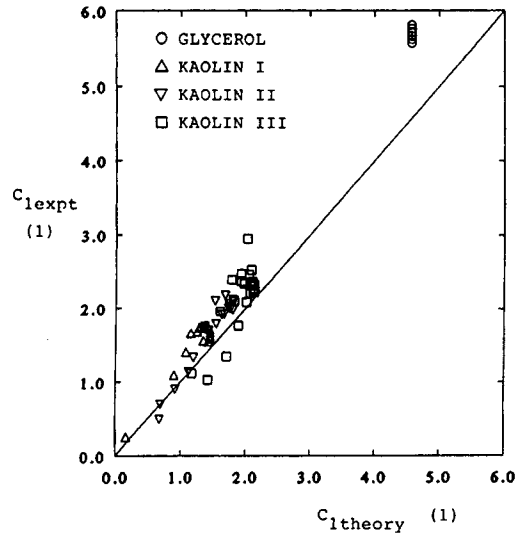

Figure 4. Experimental vs. theoretical dimensionless pressure differences and torques, first group of model fluids, gravitational flow.

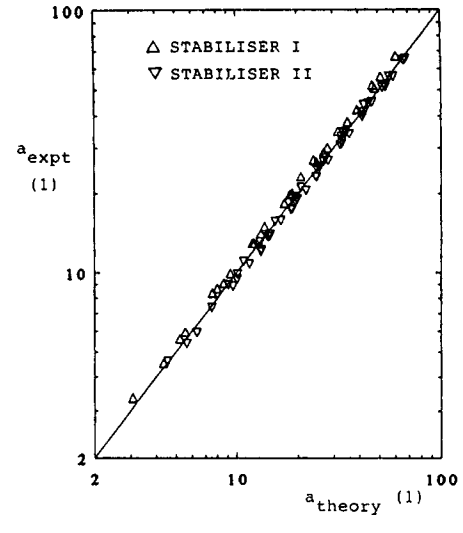

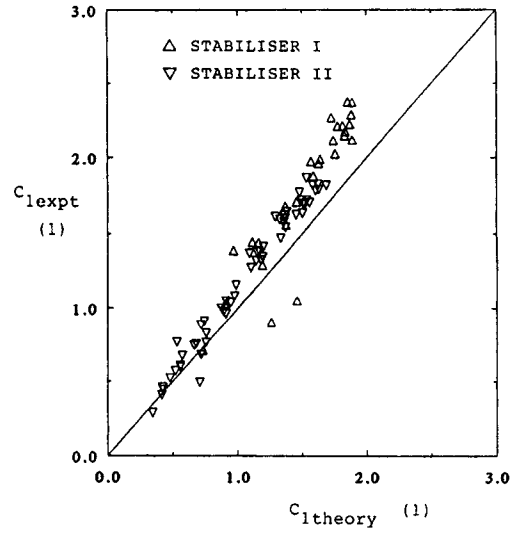

Figure 5. Experimental vs. theoretical dimensionless pressure differences and torques, second group of model fluids, flow driven by a centrifugal pump.

m = consistency coefficient, $Pa \cdot s^n$
n = flow behavior index, 1
t = temperature, °C
r = radial coordinate, m
z = axial coordinate, m
v_φ = tangential velocity, $m \cdot s^{-1}$
v_z = axial velocity, $m \cdot s^{-1}$
C_2, C_3, C_4 = integration constants, 1

Greek letters

$\dot{\gamma}_{min}$ = lowest shear rate in experiments, s^{-1}
$\dot{\gamma}_{max}$ = highest shear rate in experiments, s^{-1}
$\Delta\tau_{max}/\tau$ = maximum relative deviation of the power-law approximation in the range from $\dot{\gamma}_{min}$ to $\dot{\gamma}_{max}$, 1
τ_{ij} = shear stress, Pa
τ^*_{ij} = dimensionless shear stress, 1
ρ = density, $kg \cdot m^{-3}$
φ = angular coordinate, rad
ω = angular velocity, $rad \cdot s^{-1}$
λ = dimensionless radial coordinate, where $dv_z/dr = 0$, 1
κ = R_1/R_2 = dimensionless radii ratio, 1

Literature Cited

Bird, R. B., R. C. Armstrong, and O. Hassager, *Enhancement of Axial Annular Flow by Rotating Inner Annulus, Dynamics of Polymeric Liquids*, Vol. 1, Fluid Mechanics, Wiley, New York, pp. 226-229 (1977).

Coleman, B. D., and W. Noll, "Helical Flow of General Fluids," *J. of Appl. Phy.*, **30**, 1508 (1959).

Dierckes, A. C., and W. R. Schowalter, "Helical Flow of a Non-Newtonian Polyisobutylene Solution," *Ind. and Eng. Chem. Fund.*, **5**, 263 (1966).

Dostál, M., "Helical Flow of Non-Newtonian Fluids," M.Sc. Thesis, CTU of Prague, Faculty of Mechanical Engineering (1990).

Rea, D. R., and W. R. Schowalter, "Velocity Profiles of a Non-Newtonian Fluid in Helical Flow," *Transactions of the Society of Rheology*, **11**, pp. 125-143 (1967).

Wronski, S., M. Jastrzebski, and L. Rudniak, "Hydrodynamika laminarnego przeplywu helikoidalnego cieczy nienewtonovskich," *Inzynieria Chemiczna i Procesova*, **4**, 713 (1988).

Manuscript received Dec. 3, 1991, and revision received June 2, 1992.